Mobile Device Batteries as Thermometers

LIANG HE, University of Colorado Denver
YOUNGMOON LEE, Hanyang University
KANG G. SHIN, University of Michigan at Ann Arbor

The ability to sense ambient temperature pervasively, albeit crucial for many applications, is not yet available, causing problems such as degraded indoor thermal comfort and unexpected/premature shutoffs of mobile devices. To enable pervasive sensing of ambient temperature, we propose use of mobile device batteries as thermometers based on (i) the fact that people always carry their battery-powered smart phones, and (ii) our empirical finding that the temperature of mobile devices' batteries is highly correlated with that of their operating environment. Specifically, we design and implement *Batteries-as-Thermometers* (BaT), a temperature sensing service based on the information of mobile device batteries, expanding the ability to sense the device's ambient temperature without requiring additional sensors or taking up the limited on-device space. We have evaluated BaT on 6 Android smartphones using 19 laboratory experiments and 36 real-life field-tests, showing an average of 1.25°C error in sensing the ambient temperature.

CCS Concepts: • **Computer systems organization → Sensors and actuators**.

Additional Key Words and Phrases: mobile devices, batteries as sensors, temperature sensing

ACM Reference Format:
Liang He, Youngmoon Lee, and Kang G. Shin. 2020. Mobile Device Batteries as Thermometers. *Proc. ACM Interact. Mob. Wearable Ubiquitous Technol.* 4, 1, Article 12 (March 2020), 21 pages. https://doi.org/10.1145/3381015

1 INTRODUCTION

Sensing the ambient temperature pervasively is key to many applications, such as smart homes/buildings/cities [26, 43, 47, 50]. The ability of pervasive temperature sensing, however, is still deficient. In this paper, we propose a novel temperature sensing service, called *Batteries-as-Thermometers* (BaT), by exploiting mobile devices' batteries (and their management chips) without requiring additional sensors or taking up the limited on-device space. BaT enables mobile devices to become thermometers, thus pervasively sensing their operating ambient temperature all the time wherever we go with them. The thus-sensed temperature information can be made available to both devices and their users, enabling/improving important applications including but not limited to:

- *Indoor Thermal Map Construction.* People spend >80% of their lives inside buildings, and thus the indoor thermal comfort is crucial to their wellness/productivity [29, 35, 37, 40, 48, 54], especially in view of its spatial non-uniformity as revealed by our empirical measurements (see Fig. 1). For example, about 8% of human mortality was shown to be due to non-optimum ambient temperature according to the data collected from 384 locations during 1985–2012 [32]. The West Midlands Public Health Observatory in UK also acknowledged an increased mortality rate with ambient temperature below 20°C. Such temperature-related mortality is expected

Authors' addresses: Liang He, liang.he@ucdenver.edu, University of Colorado Denver, 1380 Lawrence Street, Denver, CO, 80204; Youngmoon Lee, youngmoonlee@hanyang.ac.kr, Hanyang University, 55 Hanyangdaehakro Sangnokgu, Ansansi, 15588; Kang G. Shin, kgshin@umich.edu, University of Michigan at Ann Arbor, 2260 Hayward St., Ann Arbor, MI, 48109-2121.

2474-9567/2020/3-ART12 $15.00
https://doi.org/10.1145/3381015

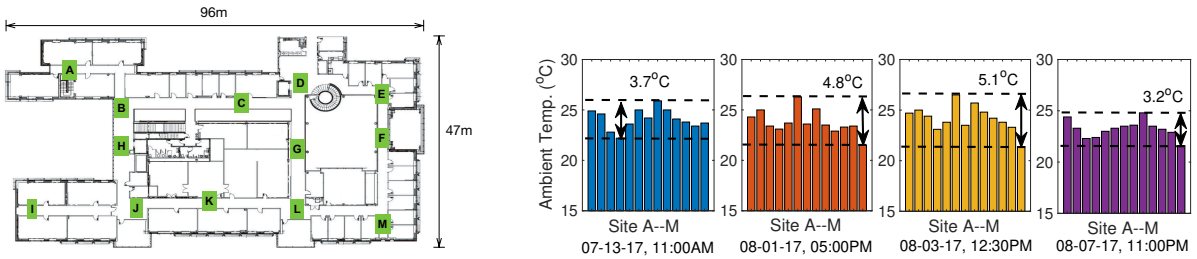

(a) Building floor map and 13 measurement sites

(b) Ambient temperature at each site differs by up to 5.1°C

Fig. 1. Non-uniform indoor temperature renders its sensing crucial to achieve occupants' indoor thermal comfort.

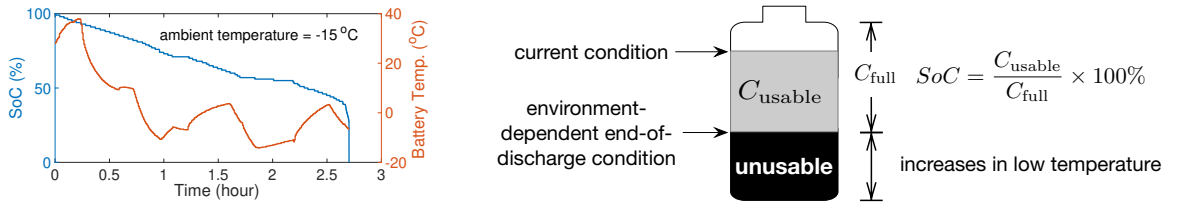

(a) Unexpected phone shutoff in cold

(b) Ambient temperature is needed to predict end-of-discharge condition

Fig. 2. Lack of ambient temperature information prevents mobile devices from predicting the end-of-discharge conditions of their batteries accurately, causing unexpected device shutoffs in a cold environment.

to rise with the rapid aging of populations [52]. BaT, by providing pervasive temperature sensing with mobile devices' batteries, not only allows occupants to acquire the temperature of their surrounding environment — e.g., by placing BaT-enabled devices in an open space like ordinary thermometers — but also facilitates (i) the construction of a building's thermal map when integrated with crowdsourcing, thus helping improve occupants' indoor thermal comfort, and (ii) detecting the malfunction of a building's heating, ventilation, and air conditioning (HVAC) system [22].

- *Environment-Aware Battery Management.* The ambient temperature of mobile devices is crucial to their operation. A cold environment reduces the temperature of device battery, causing unexpected device shutoffs, as frequently reported by mobile users on both iOS and Android platform [11, 13–15, 21]. Fig. 2(a) shows such an unexpected shutoff using an Xperia Z phone: during video streaming in a −15°C environment, the phone shut off even when it was shown to have 30% State-of-Charge (SoC). Such unexpected phone shutoffs are due to its inability to sense the environment temperature correctly, thus preventing the accurate prediction of the end-of-discharge battery conditions [7, 38] and displaying erroneous remaining SoC values, as illustrated in Fig. 2(b). On the other hand, a hot environment aggravates the heating of device battery due to impeded heat transfer from the battery to the environment, accelerating battery degradation and risking device safety. For example, we have observed overheated batteries when operating the three phones shown in Fig. 3 in a 35°C environment, where (i) Galaxy S5 and S6 Edge phones didn't shut off, but most of their services were disabled, and (ii) the Pixel XL phone completely shut off. BaT senses the devices' ambient temperature, which allows the prediction of future battery temperature in that environment, thus facilitating devices in precautiously adapting their operation to the environment to avoid/minimize the degradation of user-perceived experience.

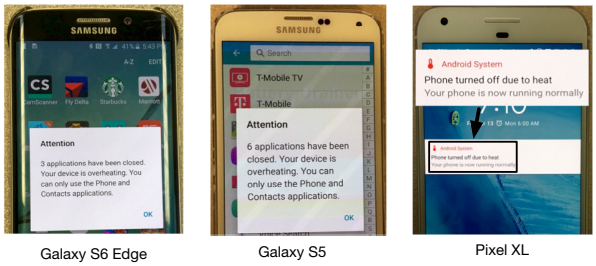

Fig. 3. Disabled phone service in a hot environment.

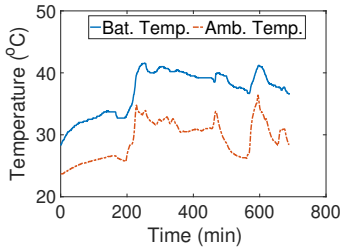

Fig. 4. The temperature of a mobile device's battery is strongly correlated with that of its ambient environment.

BaT is grounded on our empirical discovery and analytical interpretation thereof: *the temperature of a commodity mobile device battery is highly correlated with that of its ambient environment.* Fig. 4 visualizes this correlation of a Nexus 5X smartphone,[1] which we will empirically quantify further in Sec. 3. BaT captures such a correlation to estimate the device's ambient temperature, thus *"sensing"* the physical world without requiring additional thermometers or taking up the limited space on mobile devices, i.e., *sensing the temperature for free.*[2]

There are two key challenges in designing BaT.

(1) Battery temperature is affected by its current, the ambient temperature, and the heating by other phone components, such as chips or screen. Such thermal interplays have traditionally been captured analytically in electrochemical and heat transfer models [36, 51, 56, 59], which may need up to 22 describing parameters, depending on complexity/accuracy, e.g., [36]. Not all these parameters, however, are available on smart phones. To facilitate its deployability, BaT captures the battery's thermal behavior via integration of physical & data-driven modeling: (i) abstracting the electrochemical models into generalized and empirically-validated observations, and (ii) estimating the ambient temperature with such observations steered in a data-driven way.

(2) Battery could be in either *transient* or *stable* thermal state [42], according to which its correlation with devices' ambient temperature needs to be decoded differently. This is particularly critical because mobile devices' dynamic current [39], together with mobile users' frequent movements and thus change of ambients, cause device battery to make frequent state transitions. BaT identifies the battery's thermal states based on its recent temperature/current, and applies different (but closely-coupled via a control loop) techniques to estimate the ambient temperature.

We have evaluated BaT with 6 Android phones via 19 laboratory experiments and 36 real-life field-tests, and compared it with 13 off-the-shelf apps from Google Play, showing an average error of 1.25°C in sensing the ambient temperature, which is comparable to the ±2°F (or ±1.1°C) accuracy of the off-the-shelf Acurite Weather Station [1]. Such an accuracy of BaT is good enough to steer many HVAC systems to provide the indoor thermal comfort, e.g., TE-6700 Series Johnson Controls thermostat [12] keeps the indoor temperature within a ±2°F bound [22].

2 STATE OF THE ART

Below we briefly compare BaT with the state-of-the-art.

[1]The device battery's temperature was collected from its fuel-gauge chip and the ambient temperature was collected with an external Elitech RC-5 temperature logger [8].

[2]As opposed to the $3.4 cost of the temperature sensor used in, e.g., Galaxy Note 3 [6].

```
static s32 bmp085_get_temperature(struct bmp085_data *data, int
*temperature)
{
    struct bmp085_calibration_data *cali = &data->calibration;
    long x1, x2;
    int status;

    status = bmp085_update_raw_temperature(data);
    if (status != 0)
        goto exit;

    x1 = ((data->raw_temperature - cali->AC6) * cali->AC5) >> 15;
    x2 = (cali->MC << 11) / (x1 + cali->MD);
    data->b6 = x1 + x2 - 4000;
    /* if NULL just update b6. Used for pressure only measurements */
    if (temperature != NULL)
        *temperature = (x1+x2+8) >> 4;

exit:
    return status;
}
```

Fig. 5. Galaxy Note 3 estimates ambient temperature by calibrating sensor reading linearly with fixed coefficients [16].

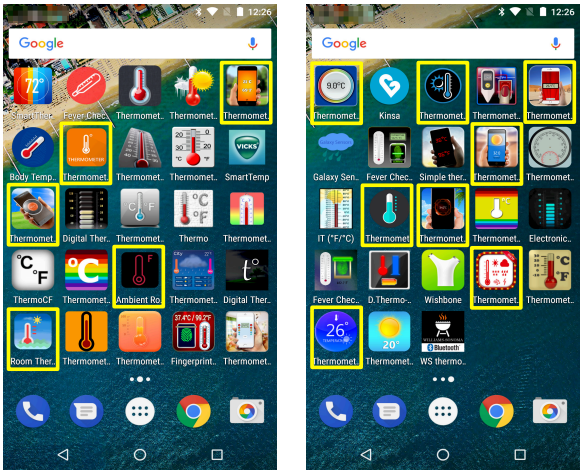

Fig. 6. Only 13 of the 48 apps could be used for ambient temperature estimation but with coarse accuracy.

• **Traditional Approaches of Temperature Sensing.** The traditional approach to deploying static thermometers for temperature sensing/monitoring [27, 34] does not work for the pervasive sensing of ambient temperature for two reasons.

(1) Ambient temperature is spatially non-uniform in both outdoor and indoor environments [44, 46]: (i) statistics show a temperature difference of up to 12°C between urban and rural outdoor areas, caused by the *urban heat island effect* [41] resulting from urbanization; (ii) the non-uniformity of indoor ambient temperature can be seen from Fig. 1, which summarizes the air temperature collected from 13 sites in our air-conditioned Department building — the temperature differs by up to 5.1°C. A temperature difference of 5.25°C in an indoor environment was also reported in [44].
(2) Humans' activities cover a large spatial area due to their frequent movements: Gonzalez *et al.* [33] reported the fact that most people travel for tens of kilometers daily, while some could regularly travel up to hundreds of kilometers, based on the trajectories of 100, 000 mobile phone users over 6 months; similar observations on human's large activity area were also reported in [57].

These two facts imply the high deployment/maintenance cost when traditional static thermometer deployment is used to monitor ambient temperature pervasively, thus rendering it ineffective.

• **BaT vs. Hardware Thermometers.** The ideal way of sensing temperature pervasively is to have everyone carry a thermometer all the time, as s/he carries a mobile phone. Inspired by this, Android provides the function of acquiring the device's ambient temperature, but such a function is applicable only when device manufactures have built hardware-based thermometers into their devices [9], as with Samsung's Galaxy S4 and Note 3 smartphones [20]. Clearly, such built-in thermometers increase the device cost (e.g., the sensor chip of Note 3 costs $3.48 apiece [6]) and take up the limited device space. Moreover, our examination of Galaxy Note 3's ambient thermometer driver [16] revealed that it just calibrates the raw thermo readings linearly with fixed coefficients (see Fig. 5), making the thus-estimated ambient temperature unreliable and suffer from up to 10°C errors [19].[3] Hardware thermometers that can be installed to mobile devices as add-on components are also available in the market, costing over $20 apiece [18].

[3]Samsung has removed these hardware thermometers in its later models.

Table 1. Classification of the 48 apps from Google Play.

Type	Description	# of apps
I	estimates body temperature based on heartbeats	6
II	returns the outdoor temperature of users' current location	11
III	requires additional hardwares/gears	9
IV	returns the reading of phone's certain thermometer	9
V	estimates based on phone's certain thermometer	13

Table 2. Error (in absolute value) of the 13 Type-V apps in estimating phones' ambient temperature.

Experiment Settings			Error of Apps (^{o}C)							
Phone	Ambient Temp.	DChg Current	#1	#2	#3	#4	#5	#6	#7	#8–#13
Nexus 5X	22^{o}C	≈ 256mA	1.1	5.6	6.1	2.1	4.1	5.1	7.4	2.6
Nexus 5X	23^{o}C	≈ 836mA	10.7	9.5	9.7	7.7	5.7	10.7	11.7	6.7
Nexus 5X	24^{o}C	≈ 1,220mA	15.1	11.0	14.1	12.1	4.1	15.1	15.4	10.9
Nexus 6P	22^{o}C	≈ 329mA	1.0	1.8	3.0	1.0	3.0	2.0	3.0	1.6
Nexus 6P	23^{o}C	≈ 600mA	9.7	7.7	8.7	6.7	2.7	9.7	10.2	5.4
Nexus 6P	24^{o}C	≈ 1,550mA	12.8	8.7	11.8	8.8	10.8	11.8	12.4	7.5

Instead of requiring additional hardware thermometers, BaT, as a (semi-)software-defined thermometer, enables mobile devices to sense, when needed, their ambient temperature using the thermometers built in their batteries, which are pervasively available on all commodity mobile devices.

• **BaT vs. Software-Defined Thermometers.** To the best of our knowledge, little has been done to explore the software-defined thermometers, i.e., extracting/estimating ambient temperature from device batteries, and the closest to BaT are [28, 42, 49]. Crowdsourcing is used in [49] to estimate the air temperature in highly populated areas. The design therein, however, only estimates daily average air temperature with coarse spatial granularity (e.g., of city level) and accuracy (e.g., up to 20% error [44]), thus making it inaccurate and also untimely. Chau has developed a method to estimate air temperature using smartphone batteries [28], which is however, applicable only to batteries that are in a stable thermal state. The temperature of mobile device battery is used to estimate/predict devices' surface temperature in [42], achieving <2^{o}C error. BaT extends further the exploration to estimate the temperature of devices' ambient.

• **BaT vs. Commercial Apps.** There exist many apps called *"thermometer"* or similar in Google Play/Apple Store. To study these apps, we installed the first 48 apps found by searching Google Play with the key word *"thermometer"* (see Fig. 6), and summarized their functionalities in Table 1 — only 13 of them (i.e., Type-V) can potentially be exploited to estimate devices' ambient temperature. To further examine the accuracy of these 13 apps (indexed as #1–#13), we ran them with varying settings as listed in Table 2. Specifically, we use an app *BatteryDrainer* [4] to regulate phones' operation (and hence control their discharge rate), and use a *Benchmark thermal chamber* [5] to control the phones' ambient temperature. The phones are placed in the chamber for 30–60 minutes, and then the estimated ambient temperature with these apps are recorded. These measurements show (i) 6 of these apps (i.e., #8–#13) always return the same estimations, and thus they are of the same estimation algorithm; (ii) these apps suffer from up to 15^{o}C error in estimating the devices' ambient temperature, especially when the discharge current is large. We will compare these apps with BaT in Sec. 6.

3 OPPORTUNITY OF USING MOBILE DEVICE BATTERIES AS THERMOMETERS

We have chosen *mobile device batteries as thermometers* for the following three reasons.

• **Readily-Available Battery Temperature.** The batteries of mobile devices are always equipped with at least one high-precision (e.g., 0.1^{o}C for Galaxy S6 Edge) thermometer to monitor their temperature in real time, to

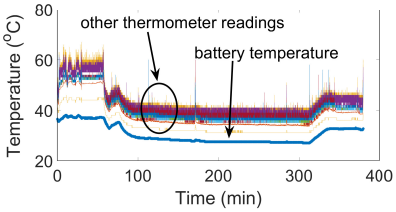

(a) Thermal readings of Nexus 5X

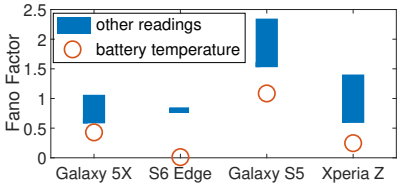

(b) Fano factors of thermal readings

Fig. 7. Battery temperature experiences less disturbance, thus being more stable than the readings of other thermometers on mobile devices.

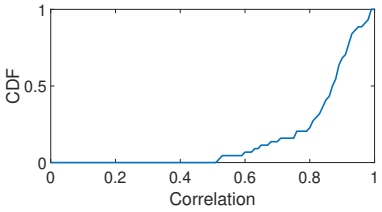

Fig. 8. 35 of the 44 pairs of battery temperature and device's ambient temperature have correlation coefficients >0.8.

ensure both energy-efficiency [55] and safety [31]. Also, the thus-collected battery temperature can be accessed on commodity platforms (i.e., Android and iOS) without requiring any privilege from users. For example, battery temperature can be accessed by reading */sys/class/power_supply/battery/temp* on Android, and via *IOKit* on iOS.

• **Reliable Battery Temperature.** Mobile devices use multiple built-in thermometers to monitor their temperature at different components/zones, e.g., batteries and chips. Of these readings, the temperature of device battery suffers less disturbance from the dynamic power usage of mobile devices and is thus more reliable (or less bursty) than others, thanks to batteries' (relatively) large thermal capacitance [59] — rendering the battery temperature a promising way to estimate the device's ambient temperature. This has been corroborated with the readings of 15 thermometers of a Nexus 5X phone (including the one for its battery) over ≈6 hours,[4] as shown in Fig. 7(a). The battery discharge current varies within [209, 1415]mA during this logging. These battery temperature measurements have a *Fano factor* — a metric widely used to quantify signal reliability — of 0.43 and a standard deviation of 3.6°C, both of which are much smaller than those of other thermo readings (i.e., 0.78–1.02 *Fano factor* and 5.7–6.7°C standard deviation), and are thus more reliable. We have also empirically verified the reliability of battery temperature with other devices, as summarized in Fig. 7(b) where the *circles* denote the Fano factor of battery temperature and the *boxes* denote the max/minimum Fano factor of other thermo readings. Note that Galaxy S6 Edge has only one more thermal reading besides the battery temperature.

• **Correlated Temperature.** The temperature of mobile device battery is strongly correlated with that of the device's ambient environment — an empirical finding from our extensive measurements. Specifically, we collected 44 traces of real-life device battery temperatures, including Nexus 6P, Nexus 5X, Galaxy S6 Edge, Galaxy S5, and Xperia Z, each lasting 1–40 hours and covering the temperature range of [14, 55]°C, over which the batteries are discharged with the current of 15–2491mA. We logged the corresponding ambient temperature at 0.1Hz for each of these measurements, ranging from 7–34°C. We calculate the cross-correlation of the thus-collected 44 pairs of battery and ambient temperatures, and observe strong correlations (with >0.8 correlation coefficients) in 35 of them, as summarized in Fig. 8.

These three facts together demonstrate the opportunity/feasibility of estimating mobile devices' ambient temperature using their battery temperatures.

4 MODEL-AIDED DESIGN PRINCIPLE

The empirically-observed correlation between battery temperature and the device's ambient temperature can be modeled analytically, which also steers BaT to estimate the ambient temperature.

[4]These readings can be accessed under */sys/class/thermal/*.

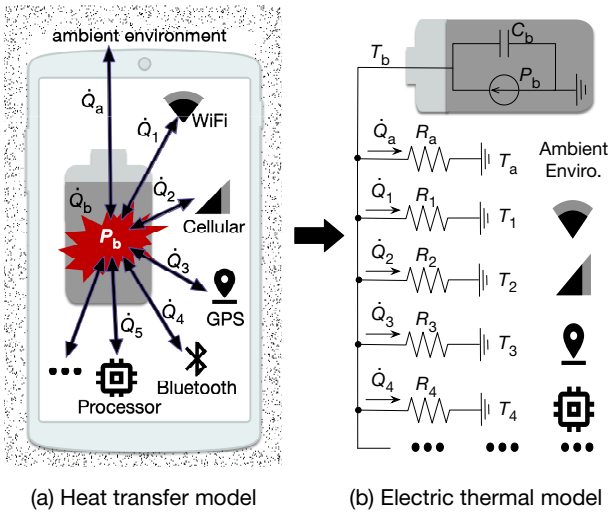

Fig. 9. Thermal model of a device battery.

• **Thermal Analysis of Device Battery.** Mobile device battery operates in a context defined by the device's ambient and other components such as processors, GPS, etc. As a result, the temperature of mobile device battery is jointly determined by its internal heating and the heat transfer from/to other device components and the ambient environment, as illustrated with a heat transfer model in Fig. 9(a), where P_b is the battery's internal heat generation, $\dot{Q}_b$ is the heat stored in the battery (i.e., as increased temperature), $\dot{Q}_a$ is the heat transfer between battery and device's ambient environment, and $\dot{Q}_i (i = 1, 2, \cdots)$ denotes the heat transfer between battery and other device components.[5] As heat conserves, we have

$$P_\mathrm{b} = \sum_i \dot{Q}_\mathrm{i} + \dot{Q}_\mathrm{b} + \dot{Q}_\mathrm{a} \; (i = 1, 2, \cdots). \tag{1}$$

This heat-transfer model can be transformed further to an electric resistance-capacitance model [25], as shown in Fig. 9(b), where the temperature difference and heat transfer rate are analogues of the electric potential and current in circuit theory, i.e., $R = \Delta T/Q$ [17]. Specifically, for Fig. 9, we know

$$\dot{Q}_\mathrm{a} = \frac{T_\mathrm{b}(t) - T_\mathrm{a}}{R_\mathrm{a}}, \tag{2}$$

$$\dot{Q}_i = \frac{T_\mathrm{b}(t) - T_i}{R_i} \; (i = 1, 2, \cdots), \tag{3}$$

where T_a, T_b, and T_i are the temperatures of ambient environment, device battery, and other device components; R_a and R_i are the thermal resistance between (i) battery and device's ambient environment and (ii) battery and other device components, capturing the heat conductivity jointly determined by the conduction coefficient and contacting surface area [25, 42].

Also, by definition, the heat stored in the battery $\dot{Q}_b$ can be captured by the battery's thermal capacitance C_b as

$$\dot{Q}_\mathrm{b} = C_\mathrm{b} \cdot dT_\mathrm{b}(t)/dt. \tag{4}$$

[5]The heat transfer could be either negative or positive.

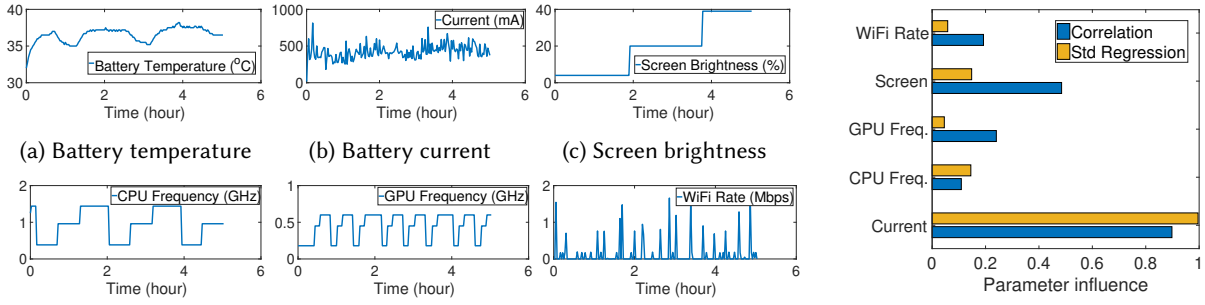

(a) Battery temperature (b) Battery current (c) Screen brightness

(d) CPU frequency (e) GPU frequency (f) WiFi data-rate (g) Impacts on battery temperature

Fig. 10. Battery current dominates the temperature of device batteries over the operation (and hence temperature) of other device components: (a)–(f) the battery current and operation details of device components during the experiment, (g) the sensitivity of battery temperature to (a)–(f).

Last but not the least, the internal heating of battery is dominated by its Ohmic heating due to its resistance r_b:

$$P_\mathrm{b}(t) = I(t)^2 \cdot r_\mathrm{b}, \tag{5}$$

where $I(t)$ is the (dis)charge current.

Combining Eqs. (1)–(5) can capture the interplay between T_a and T_b (and hence their correlation explained) by

$$I^2(t) \cdot r_\mathrm{b} = \sum_i \frac{T_\mathrm{b}(t) - T_i}{R_i} + C_\mathrm{b} \cdot \frac{dT_\mathrm{b}(t)}{dt} + \frac{T_\mathrm{b}(t) - T_\mathrm{a}}{R_\mathrm{a}}. \tag{6}$$

Moreover, Eq. (6) inspires the following three components in estimating T_a in a data-driven way.

• **Heating from Other Components $\sum(T_\mathrm{b}(t) - T_i)/R_i$.** Description of the heat transfer between battery and individual device components requires identification of R_is which, in turn, requires a significant effort. As an alternative, we have conducted sensitivity tests on T_b and empirically find that T_i's impact on T_b is dominated by that of $I(t)$. Specifically, we analyze T_b's sensitivity to individual components' operation and the aggregated I — i.e., how large does the individual components' operation and the aggregated I attribute to T_b — based on a 5-hour trace collected with a Nexus 5X phone while using *BatteryDrainer* to control the operation of the phone's major power-consuming components. Fig. 10 plots the thus-obtained results, showing $I(t)$ has a dominating impact on T_b, when compared to the other components. We have also conducted sensitivity tests on devices such as Xperia Z and Nexus 6P, and made similar observations. This is consistent with our intuition as $I(t)$ is the cumulative result of device components' operation, and thus representative to their heating effects on device batteries. More importantly, this allows BaT to estimate T_a based on only T_b and $I(t)$, i.e., shielding $T_\mathrm{i}(i = 1, 2, \cdots)$ from consideration and thus simplifying the estimation significantly. We will further experimentally validate this simplification in Sec. 6 by operating mobile devices with different loads/intensities.

• **Battery's Internal Heating $I^2(t) \cdot r_\mathrm{b}$.** The battery current is needed to capture the battery's internal heating. Current information — albeit available on most recent mobile devices, e.g., at */sys/class/power_supply/battery/* — is not always available on older or low-end devices as their fuel-gauge chips may not support current sensing, e.g., the MAX17043 chip used in 2011 Galaxy W [45]. More information on the availability/reliability of current information on different phone models can be found in [3]. For devices without current sensing capability, BaT estimates battery current based on the physical principle of $\Delta C = \int_t^{t+\Delta t} I(t)dt$, where C is capacity and I is current. This is feasible because all battery-powered devices support SoC estimation, rendering C available pervasively. Let us consider the case where the phone battery's SoC has changed from $SoC(t)$ at time t to $SoC(t + \Delta t)$ at time

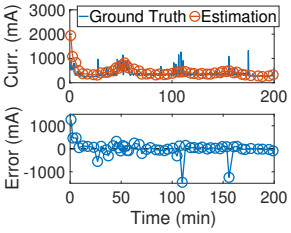

Fig. 11. Estimating current based on the changes in battery SoC.

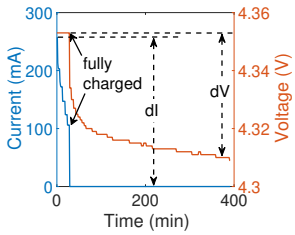

Fig. 12. Estimating battery resistance after fully charge using dV/dI.

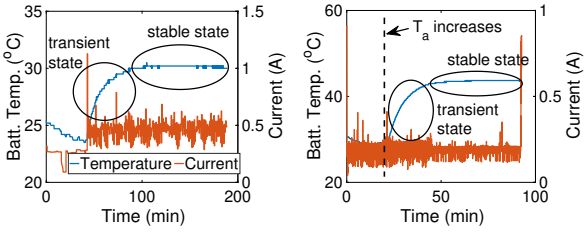

(a) With changes in I (b) With changes in T_a

Fig. 13. Battery could be in *stable* or *transient* thermal state, identification of which is needed for BaT to sense the ambient temperature.

$t + \Delta t$. Let C_0 denote the device battery's full charge capacity, e.g., 1,500mAh for Galaxy W, then the (average) battery current during time $[t, t + \Delta t]$ can be estimated as

$$\bar{I} = C_0 \cdot (SoC(t + \Delta t) - SoC(t))/(100 \cdot \Delta t), \tag{7}$$

where $\bar{I}$<0 for discharging, and otherwise charging. Fig. 11 compares the thus-estimated battery current with that provided by the fuel-gauge chip of a Nexus 5X phone, showing good accuracy except for a few large errors caused due to significant current pikes. We will further evaluate BaT's sensitivity on the error of current information in Sec. 6.

The internal heating of device battery is also affected by its resistance r. Resistance is traditionally measured based on Ohm's law (i.e., $r = dV/dI$) [53, 58, 60, 61]. Application of this principle on mobile devices, however, is non-trivial due to devices' dynamic usage patterns — the dynamic current of device battery renders it hard to quantify dV and dI reliably in practice. BaT collects reliable dV and dI by exploiting the fact that users often charge their devices over-night — the charging duration is so long that the charger is kept connected even after the device is fully charged [23, 30, 57]. This is because device chargers use separate power paths to charge the battery and power the device [24], allowing a fully charged battery to rest (i.e., with a 0mA current) if the charger is kept connected, thus making the dV/dI reliable:

$$r = \frac{dV}{dI} = \frac{V_{\text{cutoff}} - V_{\text{rested}}}{I_{\text{cutoff}} - 0} = \frac{V_{\text{cutoff}} - V_{\text{rested}}}{I_{\text{cutoff}}}, \tag{8}$$

where V_{cutoff} and I_{cutoff} are the battery voltage and charging current when stopping charging the battery, and V_{rested} is the voltage of a fully-rested battery afterwards, as illustrated in Fig. 12.

• **Battery's Thermal State $dT_b(t)/dt$.** Eq. (6) also indicates two cases of battery's thermal behavior — the *stable* or *transient* thermal state depending on whether $dT_b(t)/dt = 0$ or not. We have experimentally validated this two-state thermal behavior of device battery with a Nexus 5X phone: (i) Fig. 13(a) plots the temperature of the phone battery when its battery current increased from ≈280mA to ≈480mA with fixed ambient temperature (e.g., when the user uses the phone with a higher intensity): battery temperature rises quickly and then slowly (i.e., $|dT_b(t)/dt|$>0 and thus being in the transient state) until it converges (i.e., $|dT_b(t)/dt|$=0 and thus entering the stable state); (ii) similar two-state behaviors in battery temperature can be observed when the ambient temperature changes (e.g., when the user moves to a different environment) while keeping the battery current constant, as shown in Fig. 13(b) where the ambient temperature changes from 27°C to 40°C. Such a state-dependent thermal behavior of battery implies that the battery's real-time thermal state, besides its temperature, is also needed to estimate device's ambient temperature.

The above three observations show that: (i) it is possible to use battery current, together with its internal resistance, to (approximately) capture battery's thermal behavior; (ii) the thermal state of device batteries must

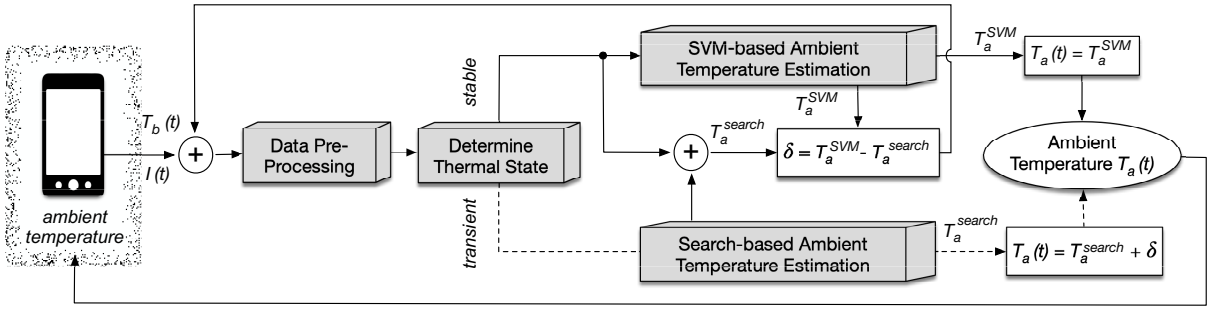

Fig. 14. BaT estimates device's ambient temperature according to battery's real-time thermal states.

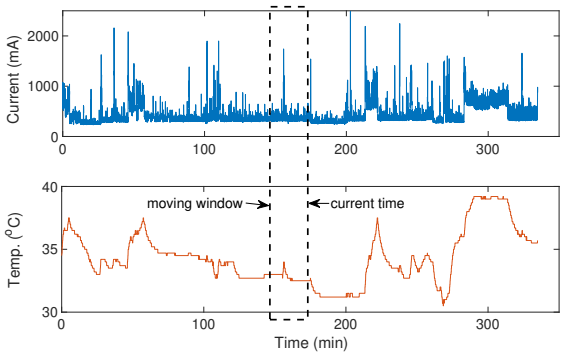

Fig. 15. BaT estimates mobile device's ambient temperature using the discharge current and temperature of its battery.

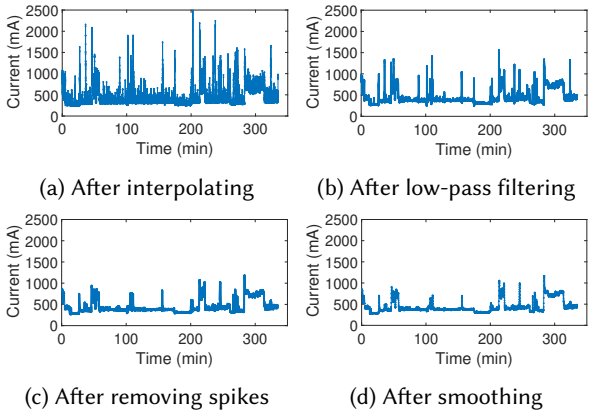

Fig. 16. Pre-processing of discharge current.

be accounted for in their thermal analysis. Steered by these, BaT estimates the ambient temperature of a mobile device using the battery current and temperature of device battery, by applying different but closely coupled data-driven approaches when the battery is in stable and transient thermal state, respectively. Note these data-driven approaches of BaT are approximation in essence, whose accuracy will be extensively validated in Sec. 6.

5 DESIGN OF BAT

Fig. 14 provides an overview of BaT with the core components shaded: collecting and processing the real-time battery information, and then identifying the thermal states of mobile device batteries to estimate the ambient temperature, such as SVM for stable-state batteries and a guided search for transient-state batteries, and connecting the two methods with a control loop.

5.1 Data Pre-Processing

BaT takes as input the recent behavior (i.e., discharge current and temperature) of mobile device battery via a moving window, as shown in Fig. 15 with a Nexus 5X phone. The pulsed battery discharge current introduces two types of noises—i.e., those with high-frequency but low-magnitude and those with low-frequency but high-magnitude—and thus needs pre-processing. BaT first interpolates the current samples linearly and then applies a 10th-order low-pass filter with 0.2Hz cutoff frequency, to remove their high-frequency but low-magnitude

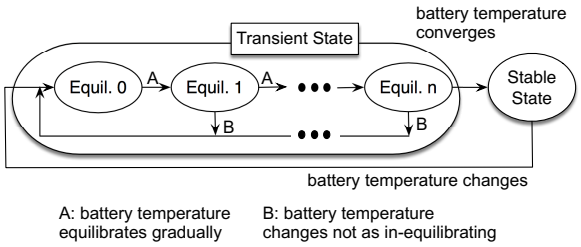

Fig. 17. Transition diagram of battery's thermal states.

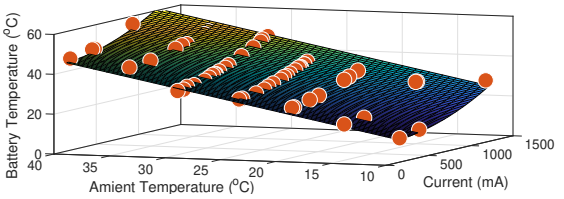

Fig. 18. The interplays among the battery's stable-state temperature T_b^{st}, ambient temperature T_a, and discharge current I fit as $T_b^{st} = a \cdot I^2 + b \cdot T_a$.

dynamics contributed probably by the device's background activities [62], which do not affect battery temperature much, as observed in Fig. 15. Also, BaT removes the top 10% of current samples in the time window to filter their spikes, possibly due to the user's brief checking of his phone which does not affect battery temperature much either due to the short duration (see Fig. 15). Finally, BaT smoothes the thus-obtained current samples with a moving average. Fig. 16 depicts these data pre-processing using the raw trace in Fig. 15.

5.2 Identifying Battery's Thermal States

BaT identifies battery's thermal state based on the collected temperature samples, as illustrated in Fig. 17: a *stable-to-transient* transition occurs if battery temperature deviates from its previously equilibrated level, i.e., $T_b(t + \Delta) - T_b(t) > \eta$ where η is an empirical threshold (e.g., η=0.1°C in our implementation of BaT on Nexus 5X, which is also the phone's precision in sensing its battery temperature), and a *transient-to-stable* transition is triggered when battery temperature converged (i.e., $T_b(t + \Delta) - T_b(t) = 0$) for a set of consecutive temperature samples. BaT then estimates the ambient temperature based on whether the device battery is stable or transient. Note that a transient battery will reset its equilibrating process if either its discharge current or ambient temperature changes again, causing its temperature to deviate from the equilibrating process, as shown with the sub-states for transient batteries in Fig. 17. We will elaborate this further in Sec. 5.4.

5.3 BaT with Stable-State Batteries

BaT, upon concluding a stable-state battery, estimates the ambient temperature with an offline-constructed SVM model describing the battery's stable-state thermal behavior. Let us consider the model construction for Nexus 5X phones as an example. We collected the stable-state battery temperature of a Nexus 5X phone, with different but constant discharge current (with `BatteryDrainer`) and ambient temperature (with the thermal chamber). We conducted 62 such experiments with $[10, 40]$°C ambient temperature, each lasting at least 1 hour to allow battery temperature to converge and thus become stable. The battery temperature and current are logged at 1Hz during these experiments. Fig. 18 summarizes the converged stable-state battery temperature T_b^{st}, together with the corresponding ambient temperature T_a and discharge current I during the experiments, from which the following observation is made.

Observation 1. *The interplays among* $<T_b^{st}, T_a, I>$ *can be captured by*

$$T_b^{st} = a \cdot I^2 + b \cdot T_a, \tag{9}$$

where a and b are regression coefficients.

Fig. 18 also plots the fitting of the collected samples according to Eq. (9), achieving a high goodness-of-fit of 0.8 RMSE and 0.9 Adjusted R-Squared. This observation can also be explained using Eq. (6) by letting $dT_b(t)/dt = 0$, i.e., when the battery is stable.

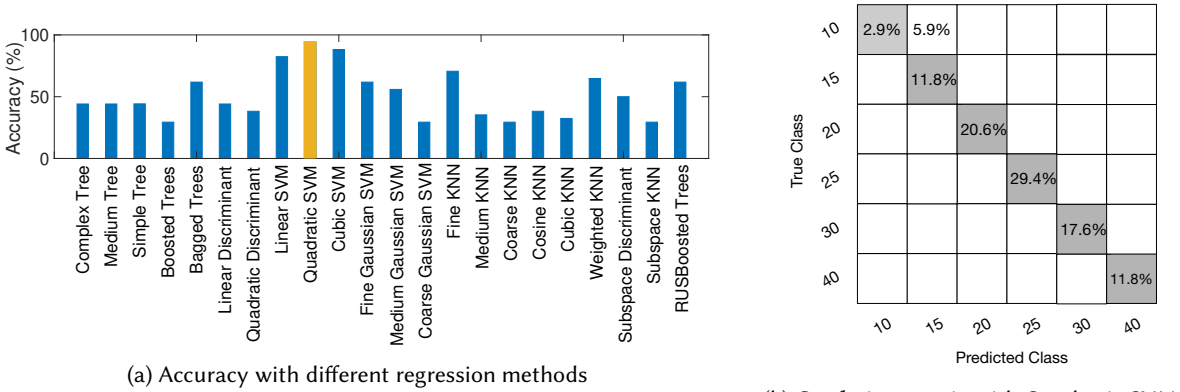

(a) Accuracy with different regression methods

(b) Confusion matrix with Quadratic SVM

Fig. 19. BaT, upon concluding a stable-state battery, estimates the ambient temperature with a Quadratic SVM model.

Inspired by Observation-1, BaT filters and smoothes the offline-collected samples using Eq. (9), and then trains a regression model with T_a as the dependent variable and $<T_b^{st}, I>$ as predictors. We tried different regression techniques as shown in Fig. 19, and found Quadratic SVM achieving the best accuracy (94%) under 5-fold cross-validation, which is not surprising because of the quadratic form of Eq. (9).

Also, the thermal behavior of device battery changes gradually over usage due to battery aging, observed as the increased internal resistance r_b and thus visible Ohmic heating, leading to an increased T_b^{st} even under the same conditions as when the training set was collected. To mitigate this, BaT, inspired by the linear effect of r_b on battery heating (i.e., $P = I^2 \cdot r_b$), calibrates the trained model according to

$$T_b^{st} = T_b^{st'} \cdot r_b / r_b', \tag{10}$$

where $T_b^{st'}$ and r_b' are the originally collected battery temperature and resistance, respectively, and r_b is the battery resistance estimated using Eq. (8). Such calibration allows BaT to collect the training set *offline*, and only *once* for a given device model. The regression model is thus agnostic of the user. To use BaT, the user *need not* perform any initial training. Also, it is critical to note that such training data set is *readily available* to device manufacturers as they have already been collecting the thermal behaviors of device batteries during their product testing (e.g., in Samsung's 8-point battery check), making BaT ideally an OEM-provided service.

Algorithm 1 BaT with transient batteries: $Trans(T_{min}, T_{max})$.

1: $\bar{T}_a = (T_{min} + T_{max})/2$;
2: predict T_b^{tr} based on $\bar{T}_a$;
3: **if** the predicted T_b^{tr} matches the collected value **then**
4: calibrate $\bar{T}_a$ based on the previous estimations with stable batteries;
5: **return** $\bar{T}_a$;
6: **else if** the predicted T_b^{tr} is larger than the collected value **then**
7: $Trans(T_{min}, (T_{min} + T_{max})/2)$;
8: **else if** the predicted T_b^{tr} is smaller than the collected value **then**
9: $Trans((T_{min} + T_{max})/2, T_{max})$;

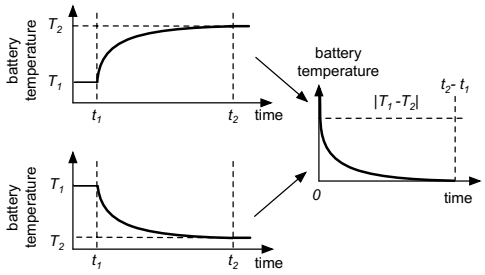

Fig. 20. Transforming the equilibrating process of battery temperature to a decaying process.

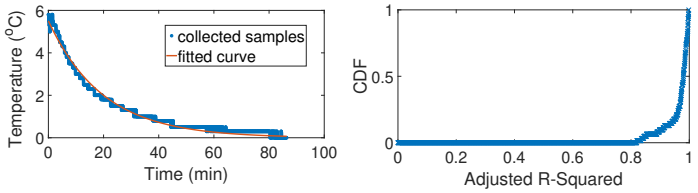

(a) Exponentially fitting (b) Fitting goodness

Fig. 21. Battery temperature equilibrates exponentially.

5.4 BaT with Transient Batteries

In practice, the battery of a mobile device switches between stable and transient state frequently, because of its dynamic usage pattern (and thus dynamic current) and the user's frequent movement (i.e., the ambient temperature is likely to change). So, BaT must also capture the thermal behavior of transient-state batteries to ensure reliable temperature sensing. The deficiency of describing transient-state batteries is also the reason why existing solutions achieve only limited accuracy, as seen from (i) Samsung's fixed linear model when estimating Note 3's ambient temperature using its built-in ambient thermometer (Fig. 5), (ii) Eq. (1) of [49], and (iii) many of the Type-V apps in Table 1 recommend to keep the phone idle for some time before using it again to ensure accuracy.

For transient batteries, BaT is steered by an empirically-learned model capturing how the battery temperature equilibrates. Specifically, BaT estimates T_a as the one matching the prediction with empirically collected battery temperature (as in the binary search of Alg. 1), which is calibrated further based on the previous estimations with stable batteries (line 4 of Alg. 1). The binary search of Alg. 1 is enabled by the monotonic relationship between T_a and T_b (see Eq. (9)). The prediction of transient battery temperature T_b^{tr} with assumed $\bar{T}_a$ (line 2 of Alg. 1) is enabled by the following observation.

Observation 2. *Battery temperature is equilibrated according to an exponential decay process:*

$$T_b^{tr}(t) = |T_b^0 - T_b^{st,1}| \cdot e^{-\lambda \cdot (t - t_0)} + T_b^{st,1} \ (t > t_0), \tag{11}$$

where t_0 and T_b^0 are the starting time of the equilibrating process and the battery temperature thereon, and $T_b^{st,1}$ is the eventually converged stable-state battery temperature (estimated based on the assumed $\bar{T}_a$, as we explain below).

Again, we corroborate this observation empirically. The equilibrating process of battery temperature — temperature rising or falling — can be transformed to a decaying process by designing the corresponding coordinate systems, as shown in Fig. 20. Fig. 21(a) plots such a decaying process of a Nexus 5X phone battery with a good exponential fit. We have collected 62 such temperature equilibrating processes and fitted them exponentially, as summarized in Fig. 21(b): the close-to-1 Adjusted R-Squared indicates high fitting accuracy. Observation-2 can also be explained analytically with Eq. (6), as elaborated in Appendix.

Observation-2 allows for estimation of $T_b^{tr}(t)$, if we know (i) the to-be-reached stable temperature $T_b^{st,1}$, (ii) the decaying rate λ, and (iii) the time since equilibrating $t - t_0$.

- **Estimating $T_b^{st,1}$.** BaT determines $T_b^{st,1}$ based on Observation-1, by assuming a known and fixed T_a.
- **Estimating λ.** BaT learns λ based on the equilibrating process it observed: estimating λ every time it sees a (sub)-equilibrating process conforming to the exponential decaying with a high goodness-of-fit. Fig. 22 plots the thus-estimated λs based on the temperature trace shown in Fig. 15, with a 30s time window: (i)

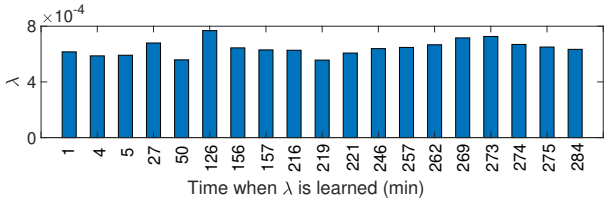

Fig. 22. Learning of λ is triggered frequently and the results are close, indicating its high availability/reliability to BaT.

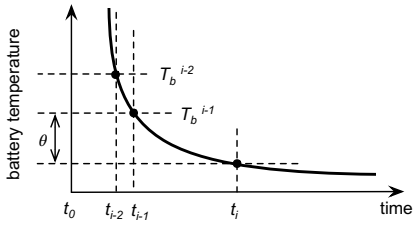

Fig. 23. BaT samples a transient battery adaptively based on how fast its temperature changes.

the estimation of λ is triggered frequently, ensuring its availability to BaT, and (ii) the estimated λs are close and thus reliable.

- **Estimating $t - t_0$.** BaT estimates $t - t_0$ by identifying the sub-state transitions for transient batteries in Fig. 17: $t = t + \Delta t$ if transition-A is triggered (i.e., if the battery temperature follows the exponential model learned since t_0 and thus changes as in the equilibration) and $t_0 = t$ if transition-B is triggered.

This way, BaT searches through the range of T_a via binary search, predicts T_b^{tr} based on each assumed T_a, and concludes the T_a that matches the predicted with empirically collected T_b^{tr} as the ambient temperature.

BaT calibrates the estimated T_a further based on the previous estimations with stable batteries, to mitigate the variance caused by the high dynamics of transient-state batteries. Specifically, BaT: (i) applies the SVM- and search-based methods upon concluding a stable battery, yielding T_a^{SVM} and T_a^{search}, respectively, (ii) estimates the ambient temperature to be T_a^{SVM}, and then (iii) uses $\delta = T_a^{SVM} - T_a^{search}$ to compensate the estimation when the battery switches to transient state later, thus connecting the two cases with a control loop. BaT updates δ when the battery becomes stable again.

5.5 Adaptive Sampling

BaT alleviates its energy overhead by sampling the device battery temperature at a reduced frequency: (i) with the device's default and low frequency (e.g., 1/30Hz for Nexus 5X) for stable batteries, and (ii) with adaptive sampling of transient battery temperature based on how fast their temperature changes — a battery only needs to be sampled when its temperature has changed by at least θ, i.e., the device's precision in sensing battery temperature. Specifically, for transient batteries, BaT predicts the cumulative change of θ in battery temperature using Eq. (11) (as illustrated in Fig. 23), and samples the battery temperature at that time. Let T_b^{i-2} and T_b^{i-1} be the battery temperature at time t_{i-2} and t_{i-1} when the $(i-2)$-th and $(i-1)$-th samples are collected. BaT takes the i-th sample at time

$$t_i = -\frac{1}{\lambda} \cdot \ln[(1 + \frac{\theta}{T_b^{i-2} - T_b^{i-1}}) \cdot e^{-\lambda \cdot (t_{i-1} - t_0)} - \frac{\theta}{T_b^{i-2} - T_b^{i-1}} \cdot e^{-\lambda \cdot (t_{i-2} - t_0)}] + t_0. \quad (12)$$

6 EVALUATION

We have evaluated BaT using both laboratory experiments and field-tests with 6 smartphones: 2 Nexus 5X, 1 Nexus 6P, 1 Galaxy S6 Edge, 1 Xperia Z, and 1 Pixel XL. The current information of Nexus 6P, Nexus 5X, Galaxy S6 Edge, and Xperia Z is collected by reading */sys/class/power_supply/battery/current_now*, and that of Pixel XL is estimated according to Eq. (7).

Table 3. Experimental comparison of BaT with the 13 Type-V apps in Table 1.

Settings			Error of Apps (°C)								
Test ID	**Amb. T.**	**Curr.**	BaT	**#1**	**#2**	**#3**	**#4**	**#5**	**#6**	**#7**	**#8–#13**
#1	16°C	471mA	0.5	6.0	6.8	5.0	3.0	-3.0	6.0	7.5	3.0
#2	16°C	763mA	0.2	13.0	16.2	12.0	11.0	13.0	14.0	15.0	10.2
#3	20°C	803mA	1.4	10.0	10.4	9.0	7.0	14.0	10.0	11.2	6.4
#4	21°C	279mA	0.1	-2.0	-0.1	-3.0	-3.0	-1.0	3.0	4.3	-0.3
#5	21°C	542mA	0.7	0	-0.5	2.0	-1.0	1.0	3.0	4.8	0.1
#6	22°C	819mA	1.0	10.0	3.8	9.0	7.0	9.0	10.0	10.8	6.0
#7	22°C	836mA	-0.5	10.7	9.5	9.7	7.7	5.7	10.7	11.7	6.7
#8	23°C	256mA	0.6	1.1	5.6	6.1	2.1	4.1	5.1	7.4	2.6
#9	24°C	1220mA	1.1	15.0	10.9	14.0	12.0	4.0	15.0	15.3	10.8
#10	25°C	283mA	-0.9	1.0	2.2	2.0	-2.0	0	1.0	2.1	-2.6
#11	25°C	575mA	0.6	5.0	4.3	4.0	2.0	4.0	5.0	6.6	1.8
#12	25°C	678mA	0.3	10.0	7.8	9.0	7.0	9.0	10.0	11.0	4.7
#13	30°C	346mA	-0.7	-1.0	-3.0	-2.0	-4.0	1.0	0	0.7	-4.1
#14	30°C	442mA	0.3	3.0	0	3.0	0	1.0	4.0	4.2	-0.7
#15	30°C	615mA	1.1	7.0	3.3	6.0	4.0	6.0	7.0	7.5	2.0
#16	35°C	680mA	-0.8	6.0	2.7	5.0	3.0	5.0	6.0	5.5	0.5
#17	35°C	704mA	0.5	9.0	8.3	8.0	6.0	5.0	8.0	7.4	2.5
#18	40°C	343mA	-0.5	1.0	-2.3	1.0	-2.0	1.0	1.0	1.6	-4.3
#19	40°C	639mA	0.3	6.0	4.6	5.0	3.0	0	6.0	4.0	-0.9
Overall Range			[-0.9, 1.4]	[-2, 15]	[-3, 16.2]	[-3, 14]	[-4, 12]	[-3, 14]	[0, 15]	[0.7, 15.3]	[-4.3, 10.8]
Mean of Absolute Error			0.63	6.15	5.38	6.04	4.57	4.57	6.57	7.29	3.69
Standard Deviation			0.68	4.96	4.99	4.46	4.63	4.60	4.24	4.26	4.31

Table 4. Summary of tests in common usage scenarios.

Scenario	Current	Battery Temp.	Duration
Idling	28–602mA	22–32°C	2.5–15 hours
Listening-to-Music	324–991mA	22–33°C	1.1–2 hours
Youtubing	214–1,317mA	24–38°C	0.9–2.8 hours
Gaming	438–1,091mA	25–45°C	0.8–1.2 hours

6.1 Comparison with Off-the-Shelf Apps

We first compared BaT with the 13 Type-V apps in Table 1 via 19 laboratory experiments. Again, we use *BatteryDrainer* to regulate the discharge rate of a Nexus 5X phone at a (relatively) fixed level, and use the thermal chamber to control the ambient temperature. The ambient temperature is estimated after putting the phone in the chamber for 30–60 minutes to allow the equilibration of battery temperature. Table 3 summarizes the estimation errors obtained with BaT and the 13 apps, together with the corresponding ground truth of ambient temperature and the phone's discharge current during the experiments. BaT senses the ambient temperature with errors in $[-0.9, 1.4]$°C across all the 19 cases and an average of 0.64°C, which is much more accurate than these apps and is comparable to the ±2°F (or ±1.1°C) accuracy of the off-the-shelf Acurite Weather Station [1].

6.2 BaT in Common Usage Scenarios

We have evaluated BaT when the phones operate in scenarios commonly seen by phone users, i.e., *idling*, *listening-to-music*, *Youtubing*, and *gaming*. The app of *Amazon Music* [2] is used when listening to music online with screen off and an earphone, and *Fishdom* [10], a game requiring intensive human-phone interactions with over 10 million downloads on Google Play, is used for the gaming scenario. The phones operate with different components & intensities in these scenarios, facilitating validation of BaT's simplification of excluding T_is in Eq. (6) from its temperature sensing. The phones are placed on a desk during these experiments. The Elitech RC-5 thermal loggers are placed near (but not in contacting with) the phones to collect the true ambient temperature. Table 4

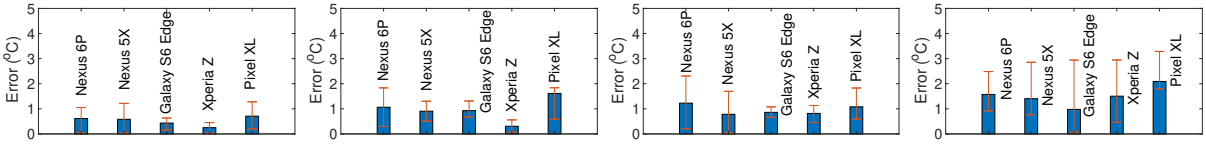

(a) Idling (b) Listening to music (c) Youtubing (d) Gaming

Fig. 24. BaT's accuracy in estimating the ambient temperature of phones under common usage scenarios.

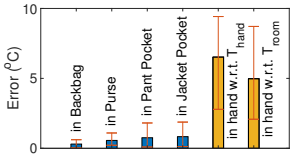

Fig. 25. BaT's accuracy at different contexts.

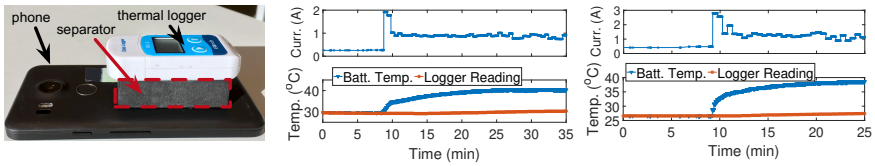

(a) A separator is inserted (b) w/ Nexus 5X (c) w/ Nexus 6P

Fig. 26. A heat separator is inserted between the phone and the logger to reduce the disturbance of the logger's readings caused by the phone's heating.

summarizes the phones' discharge current and battery temperature during these experiments and the durations thereof. The maximum currents of 602/991mA with idle/listening-to-music phones are incurred when the screen is turned on to start/terminate the experiments. Fig. 24 plots the accuracy of BaT in estimating the phones' ambient temperature obtained in these experiments, in terms of the 10-th, mean, and 90-th percentiles of the absolute estimation errors. BaT achieves 0.25-0.7°C mean estimation errors with idle phones, and even the 90-th percentile of the error is below 1.3°C. The estimation error increases in scenarios of *listening-to-music*, *Youtubing*, and *gaming*, because of the larger and more dynamic currents, especially for the gaming scenario with frequent user–device interactions, but the error is still below 2.1/3.3°C for the 50/90-th percentiles.

6.3 BaT with Common Device Placements

The phones are kept on a desk in the above experiments. We have further evaluated BaT's accuracy when the devices are placed at other common places, i.e., *in backpack*, *in handbag*, *in pant/jacket pocket*, and *in hand*. Fig. 25 plots the results collected with a Nexus 5X phone, where each experiment lasts 50-140 minutes. The temperature inside the backpack/handbag/pockets, collected with a thermal logger, is taken as the ground truth in the corresponding experiments, in which cases BaT achieves an average error of less than 0.85°C. The case of holding the phone in hand, however, is tricky because of the lack of clear definition of the phone's operating ambient environment — it will be a combination of the holding hand and the surrounding air. We have used (i) the temperature of the holding hand, and (ii) the air temperature of the room in which the experiment is conducted, as the upper and lower bounds of the ground truth, respectively. As expected, BaT under/over-estimates the ambient temperature, when it is (approximately) defined as the temperature of hand/room, respectively.

6.4 BaT in Real-Life Usage

After validating BaT's performance in specific scenarios/ambient, we next evaluate BaT with 36 real-life field-tests, i.e., using BaT to estimate, in real time, the phones' ambient temperature during their daily usage. These field-tests cover different phone usage patterns and ambient changes, e.g, when the user moves from an air-conditioned office to an outdoor park in summer afternoons. Each of these field-tests lasts 4–22 hours, during which the

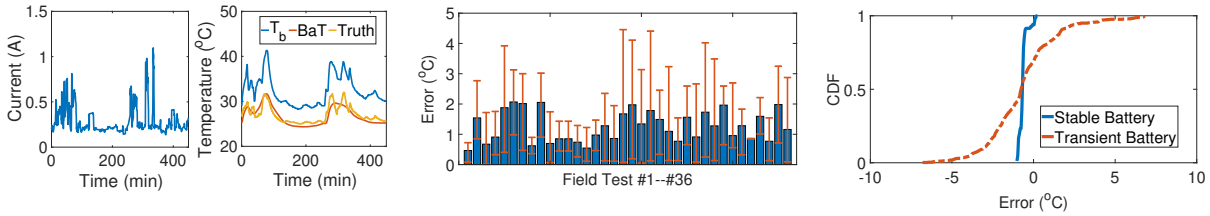

(a) Exemplary field-test results (b) Summary of results (c) Transient v.s. stable batteries

Fig. 27. We have evaluated BaT with 36 real life field-tests, showing (i) BaT senses the ambient temperature with average errors of 0.46–2.07°C, and (ii) BaT achieves much better accuracy when the batteries of mobile devices are stable.

discharge current, battery temperature, and ambient temperature vary from 152–2, 491mA, 12–55°C, and 6–41°C, respectively.

We attached the Elitech RC-5 thermal loggers to the phones to collect the ground truth of phones' ambient temperature at 0.1Hz, with a $2.5'' \times 1.1'' \times 0.6''$ heat separator in between to reduce the disturbance caused by the phone's heating, as shown in Fig. 26(a). We have validated the effectiveness of the heat separator with the Nexus 5X and 6P phones, as plotted in Figs. 26(b) and (c): the logger's readings are insensitive to the dramatically increased discharge current (and hence battery temperature), validating the reliability of the thus-collected ground truth. The attachment of logger/separator to the phones, albeit increasing the physical size, is acceptable for the field-tests as the phones may still be held in hand easily. Also note that the logger/separator are only for the collection of ground truth and are not needed when deploying BaT in the real-world.

Fig. 27(a) plots one such field-test with a Nexus 5X phone, including (i) the battery information collected during the ≈7.5-hour test, and (ii) the thus-estimated ambient temperature which is further smoothed with moving average, together with the collected ground truth of ambient temperature for comparison. The phone was kept at different places such as *in pocket*, *in bag*, *in hand*, and *on desk* during this test, and the user's activities include *working in office*, *driving*, *running in a park*, and *at home*. Note this field-test covers many transition scenarios in which the phone's ambient temperature changes because of the user's activities, e.g., returning to home after running in a park. BaT estimates the ambient temperature with a mean error of 1.07°C and with 10-th and 90-th percentiles of 0.29°C and 2.06°C, respectively. Also, BaT achieves a smaller estimation error when the battery temperature is relatively stable, as compared to transient state batteries. Fig. 27(a) also shows that estimating the ambient temperature simply to be that of the device battery — like some of the Type-IV apps in Table 1 — is not accurate. Moreover, even estimating the ambient temperature by shifting the battery temperature with a posteriori-identified optimal offset leads to an averaged estimation error of 2.25°C and a 90-th percentile of 5.02°C, which are much larger than BaT. Fig. 27(b) summarizes the estimation errors for each of these 36 field-tests, ranging from 0.46–2.07°C. An overall mean error of 1.25°C is achieved across all the tests, with an average 90-th percentile of 2.44°C.

To further examine BaT's accuracy with stable and transient batteries, we categorize its estimations of ambient temperature based on the battery's thermal state. Fig. 27(c) plots the CDFs of the estimation errors in these two cases, showing BaT achieves an average estimation error of 1.76°C when the phone battery is in transient-state, which reduces further to 0.54°C for stable batteries. This also implies that ensuring a stable device battery is an effective direction to improve BaT's accuracy further.

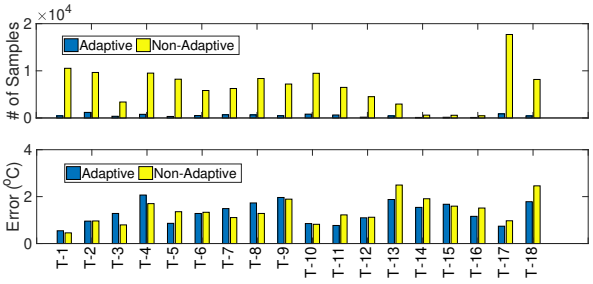

Fig. 28. Adaptive sampling reduces sampling overhead without degrading accuracy of ambient temperature estimation.

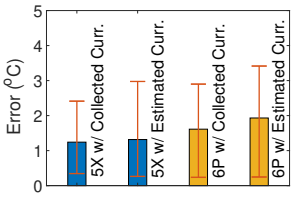

Fig. 29. BaT's accuracy with current (i) reported by fuel-gauge chips and (ii) estimated based on battery SoC.

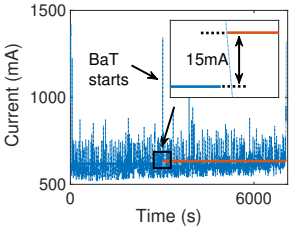

Fig. 30. BaT incurs only about 15mA energy overhead even without the adaptive sampling.

6.5 Effectiveness of Adaptive Sampling

BaT adaptively samples the battery information to reduce its energy overhead, by focusing only on crucial battery thermal behaviors. Fig. 28 compares BaT's performance with and without adaptive sampling using 18 tests, in terms of sampling overhead and estimation accuracy, respectively. The battery information is sampled at 0.2Hz in case of non-adaptive sampling. Adaptive sampling reduces the number of samples by about 75–97%, when compared with the case of a fixed sampling rate, significantly reduces BaT's overhead. Moreover, adaptive sampling causes no clear accuracy degradation in estimating the ambient temperature — it leads to estimation errors of about 0.6–1.6x of that when sampling constantly, with an average of 0.99x across all tests.

6.6 Accuracy with Estimated Current

To further check BaT's deployability on phones without current sensing capability, we implement BaT based on the discharge current (i) reported by phones' fuel-gauge chips and (ii) estimated based on battery SoC (i.e., Eq. (7)), with a Nexus 5X and a Nexus 6P phone. Fig. 29 plots the thus-obtained results: the estimated current only slightly degrades BaT's accuracy when compared to the current measured by the chip, demonstrating BaT's pervasive deployability.

6.7 Overhead Analysis

To quantify BaT's energy overhead, we logged the battery current of an idle Xperia Z phone for about 50 minutes with all other services/apps disabled, and then start BaT and log the discharge current for another 70 minutes. This way, the difference between the discharge currents in the two cases will be the energy overhead of BaT. Note that to reduce the randomness of the thus-measured energy consumption, the adaptive sampling of BaT is *disabled* and a fixed sampling rate of 1/30Hz — which is much higher than that with the adaptive sampling — is used in this experiment. Fig. 30 plots the thus-collected current trace, where the high spikes are caused by human interactions when starting/switching/terminating the experiment: BaT causes only a 15mA increase in discharge current even without adaptive sampling.

7 CONCLUSIONS

In this paper, we have designed and implemented BaT to sense mobile devices' operating ambient temperature using their batteries, expanding the ability to sense the physical world pervasively without requiring additional thermometers. BaT is inspired by (i) the fact that people always carry their mobile devices, and (ii) our empirical finding that the temperature of device battery correlates highly with that of devices' ambient temperature. We have evaluated BaT using both laboratory experiments and field-tests on multiple Android devices, showing an

average of 1.25°C error in sensing ambient temperature. Such an accuracy of BaT is sufficient to steer many applications such as facilitating the environment-aware battery management for mobile devices or helping users find their comfort areas in a building.

ACKNOWLEDGMENTS

We would like to thank the anonymous reviewers for constructive suggestions. The work reported in this paper was supported by NSF under Grant CNS-1446117 and CNS-1739577.

REFERENCES

[1] 2019. Acurite Weather Station. https://www.acurite.com/.
[2] 2019. Amazon Music. https://play.google.com/store/apps/details?id=com.amazon.mp3.
[3] 2019. Ampere the charging meter. http://forum.xda-developers.com/android/apps-games/app-ampere-charging-meter-t3012890.
[4] 2019. Battery Drainer. https://play.google.com/store/apps/details?id=mertcancucen.com.YourBatteryDrainer.
[5] 2019. Benchmark Thermo Chamber. http://www.benchmarkscientific.com/MyTemp.html.
[6] 2019. Cost of temperature sensor SHTC1. https://www.digikey.com/product-detail/en/sensirion-ag/SHTC1/1649-1015-1-ND/5872297.
[7] 2019. Discharging at High and Low Temperatures. http://batteryuniversity.com/learn/article/discharging_at_high_and_low_temperatures.
[8] 2019. Elitech RC-5 Thermal Logger. http://www.elitechus.com.
[9] 2019. Environment Sensors. https://developer.android.com/guide/topics/sensors/sensors_environment.html.
[10] 2019. Fishdom. https://play.google.com/store/apps/details?id=com.playrix.fishdomdd. gplay&hl=en.
[11] 2019. iPhone 5 Shutting down, Cold Weather or defective battery. https://discussions.apple.com/thread/4742928?tstart=0 .
[12] 2019. Johnson Controls Inc. TE-6700 Series 2nd Generation Temperature Elements. http://cgproducts.johnsoncontrols.com/met_pdf/216331.pdf.
[13] 2019. Nexus 6P goes from 15% to 0% almost straight away. https://productforums.google.com/forum/#!topic/nexus/SeB67voFk38.
[14] 2019. Samsung Galaxy S4 turns off but still has 30% battery life. http://forums.androidcentral.com/samsung-galaxy-s4/303065-samsung-galaxy-s4-turns-off-but-still-has-30-battery-life.html.
[15] 2019. Sub-Zero Weather: Can Your Smartphone Stand The Cold? http://www.pcworld.com/article/249134/sub_zero_weather_can_your_smartphone_stand_the_cold_.html.
[16] 2019. Temperature sensor driver for SHTC1. https://android.googlesource.com/kernel/msm/+/android-7.1.0_r0.2/drivers/hwmon/shtc1.c
[17] 2019. Thermal-electrical analogy: thermal network. http://www.ingaero.uniroma1.it/attachments/2176_Cap_3%20Thermal-electrical%20analogy.pdf.
[18] 2019. Thermodo. http://thermodo.com/.
[19] 2019. Thermometer accuracy. https://forums.androidcentral.com/samsung-galaxy-s4/278311-thermometer-accuracy.html.
[20] 2019. Turn Your Samsung Galaxy Note 3 into a Personal Ambient Weather Station. https://galaxy-note-3.gadgethacks.com/how-to/turn-your-samsung-galaxy-note-3-into-personal-ambient-weather-station-with-these-apps-widgets-0149784/.
[21] Hoque Mohammad A. and Tarkoma Sasu. 2015. Understanding Smartphone State of Charge Anomaly. In *HotPower'15*.
[22] Bharathan Balaji, Jason Koh, Nadir Weibel, and Yuvraj Agarwal. 2016. Genie: A Longitudinal Study Comparing Physical and Software Thermostats in Office Buildings. In *UbiComp'16*.
[23] Nilanjan Banerjee, Ahmad Rahmati, Mark Corner, Sami Rollins, and Lin Zhong. 2007. Users and Batteries : Interactions and Adaptive Energy Management in Mobile Systems. In *Ubicomp'07*.
[24] Yevgen Barsukov and Jinrong Qian. 2013. Battery power management for portable devices. *Artech House* (2013), 67.
[25] Theodore L. Bergman, Adrienne S. Lavine, Frank P. Incropera, and David P. Dewitt. 2011. *Fundamentals of Heat and Mass Transfer. 7th Edition*. 1048 pages. https://doi.org/10.1007/s13398-014-0173-7.2 arXiv:arXiv:1011.1669v3
[26] Rachel Cardell-Oliver and Chayan Sarkar. 2017. BuildSense: Long-term, fine-grained building monitoring with minimal sensor infrastructure. In *BuildSys'17*.
[27] M. Ceriotti, L. Mottola, G. P. Picco, A. L. Murphy, S. Guna, M. Corra, M. Pozzi, D. Zonta, and P. Zanon. 2009. Monitoring heritage buildings with wireless sensor networks: The Torre Aquila deployment. In *IPSN'09*.
[28] Hguyen Hai Chau. 2019. Estimation of air temperature using smartphones in different contexts. *Journal of Information and Telecommunication* 3, 4 (2019), 494–507.
[29] P. O. Fanger. 1970. *Thermal comfort. Analysis and applications in environmental engineering*. Danish Technical Press.
[30] Denzil Ferreira, Anind Dey, and Vassilis Kostakos. 2011. Understand Human-smartphone Concerns: A Study of Battery Life. In *Pervasive'11*.

[31] Donal Finegan, Mario Scheel, James Robinson, Bernhard Tjaden, Marco Michiel, Gareth Hinds, Dan Brett, and Paul Shearing. 2016. Investigating Li-ion battery materials during overcharge-induced thermal runaway: an operando and multi-scale X-ray CT study. *Phys. Chem. Chem. Phys.* (2016).
[32] Antonio Gasparrini, Yuming Guo, Masahiro Hashizume, Eric Lavigne, Antonella Zanobetti, Joel Schwartz, Aurelio Tobias, Shilu Tong, Joacim Rocklöv, Bertil Forsberg, Michela Leone, Manuela De Sario, Michelle L Bell, Yue-Liang Leon Guo, Chang-fu Wu, Haidong Kan, Seung-Muk Yi, Micheline de Sousa Zanotti Stagliorio Coelho, Paulo Hilario Nascimento Saldiva, Yasushi Honda, Ho Kim, and Ben Armstrong. 2017. Mortality risk attributable to high and low ambient temperature: a multicountry observational study. *The Lancet* 386, 9991 (2017), 369–375.
[33] Marta C. Gonzalez, Cesar A. Hidalgo, and Albert-Laszlo Barabasi. 2008. Understanding individual human mobility patterns. *Nature* 453 (2008), 779–782.
[34] S. Grassini, E. Angelini, A. Elsayed, S. Corbellini, L. Lombardo, and M. Parvis. 2017. Cloud infrastructure for museum environmental monitoring. In *I2MTC*.
[35] Vivek Gupta, Siddhant Mittal, Sandip Bhaumik, and Raj Roy. 2016. Assisting humans to achieve optimal sleep by changing ambient temperature. In *BIBM'16*.
[36] S. Al Hallaj, H. Maleki, J.S. Hong, and J.R. Selman. 1999. Thermal modeling and design considerations of lithium-ion batteries. *Journal of Power Sources* 83, 1 (1999), 1 – 8.
[37] E.H Haskell, J.W Palca, J.M Walker, R.J Berger, and H.C Heller. 1981. The effects of high and low ambient temperatures on human sleep stages. *Electroencephalography and Clinical Neurophysiology* 51, 5 (1981), 494 – 501.
[38] Liang He, Youngmoon Lee, Eugene Kim, and Kang G. Shin. 2019. Environment-Aware Estimation of Battery State-of-Charge for Mobile Devices. In *ICCPS'19*.
[39] L. He, G. Meng, Y. Gu, C. Liu, J. Sun, T. Zhu, Y. Liu, and K. G. Shin. 2017. Battery-aware mobile data service. *IEEE Transactions on Mobile Computing* 6, 16 (2017), 1544–1558.
[40] Alan Hedge. 2004. Linking Environmental Conditions to Productivity. In *EECS'04*.
[41] Aurelien Kaiser, Thomas Merckx, and Hans Van Dyck. 2016. The Urban Heat Island and its spatial scale dependent impact on survival and development in butterflies of different thermal sensitivity. *Ecology and Evolution* 6, 12 (2016), 4129–4140.
[42] Soowon Kang, Hyeonwoo Choi, Sooyoung Park, Chunjong Park, Jemin Lee, Uichin Lee, and Sung-Ju Lee. 2019. Fire in Your Hands: Understanding Thermal Behavior of Smartphones. In *MobiCom?19*.
[43] Amine Lazrak and Michael Zeifman. 2017. Estimation of Physical Buildings Parameters Using Interval Thermostat Data. In *BuildSys'17*.
[44] R. Majethia, V. Mishra, P. Pathak, D. Lohani, D. Acharya, and S. Sehrawat. 2015. Contextual sensitivity of the ambient temperature sensor in Smartphones. In *COMSNETS'15*.
[45] MAX17043. 2017. 1-Cell/2-Cell Fuel Gauge with ModelGauge and Low-Battery Alert. *Maximum Integrated* (2017).
[46] Maria Mookken, P.M.Joy, and Nishad Narayanan. 2011. Analysis of spatial variation of ambient air temperature. *Geospatial World* (2011).
[47] Paolo Neirotti, Alberto De Marco, Anna Corinna Cagliano, Giulio Mangano, and Francesco Scorrano. 2014. Current trends in Smart City initiatives: Some stylised facts. *Cities* 38 (2014), 25 – 36.
[48] J.F. Nicol and M.A. Humphreys. 2002. Adaptive thermal comfort and sustainable thermal standards for buildings. *Energy and Buildings* 34, 6 (2002), 563 – 572.
[49] A. Overeem, J. C. R. Robinson, H. Leijnse, G. J. Steeneveld, B. K. P. Horn, and R. Uijlenhoet. 2013. Crowdsourcing urban air temperatures from smartphone battery temperatures. *Geophysical Research Letters* 40, 15 (2013), 4081–4085.
[50] M. A. A. Pedrasa, T. D. Spooner, and I. F. MacGill. 2010. Coordinated Scheduling of Residential Distributed Energy Resources to Optimize Smart Home Energy Services. *IEEE Transactions on Smart Grid* 1, 2 (2010), 134–143.
[51] Ahmadou Samba, Noshin Omar, Hamid Gualous, Youssef Firouz, Peter Van den Bossche, Joeri Van Mierlo, and Tala Ighil Boubekeur. 2014. Development of an Advanced Two-Dimensional Thermal Model for Large size Lithium-ion Pouch Cells. *Electrochimica Acta* 117, Supplement C (2014), 246 – 254.
[52] A Schneider and S. Breitner. 2016. Temperature effects on health – current findings and future implications. *EBioMedicine* 6 (2016), 29–30.
[53] Hans-Georg Schweiger, Soosma Obidi, Oliver Komesker, Andre Raschke, Michael Schiemann, Christian Zehner, Markus Gehnen, Michael Keller, and Peter Birke. 2010. Comparison of several methods for determining the internal resistance of Lithium ion cells. *Sensors* 10 (2010), 5604 – 5625.
[54] Cong Song, Yanfeng Liu, Xiaojun Zhou, and Jiaping Liu. 2015. Investigation of Human Thermal Comfort in Sleeping Environments Based on the Effects of Bed Climate. *Procedia Eng.* 121, Supplement C (2015), 1126 – 1132.
[55] Haishen Song, Zheng Cao an Xiong Chen, Hai Lu, Ming Jia, Zhian Zhang, yanqing Lai, Jie Li, and Yexiang Liu. 2013. Capacity fade of $LiFePO_4$/graphite cell at elevated temperature. *Journal of Solid State Electrochem* 17 (2013), 599–605.
[56] Peyman Taheri, Maryam Yazdanpour, and Majid Bahrami. 2013. Transient three-dimensional thermal model for batteries with thin electrodes. *J. of Power Sources* 243, Supplement C (2013), 280 – 289.

[57] Daniel Wagner, Andrew Rice, and Alastair Beresford. 2013. Device Analyzer: Understanding smartphone usage. In *MOBIQUITOUS'13*.
[58] Xiaogang Wu, Zhe Chen, and Zhiyang Wang. 2017. Analysis of Low Temperature Preheating Effect Based on Battery Temperature-Rise Model. *Energies* 10, 8 (2017).
[59] Q. Xie, J. Kim, Y. Wang, D. Shin, N. Chang, and M. Pedram. 2013. Dynamic thermal management in mobile devices considering the thermal coupling between battery and application processor. In *ICCAD'13*.
[60] Fengyuan Xu, Yunxin Liu, Qun Li, and Yongguang Zhang. 2013. V-edge: Fast Self-constructive Power Modeling of Smartphones Based on Battery Voltage Dynamics. In *NSDI'13*.
[61] Ming Yu, Yevgen Barsukov, and Michael Vega. 2008. Theory and Implementation of Impedance Track Battery Fuel-Gauging Algorithm in bq2750x Family. *Application Report, SLUA450* (2008).
[62] Ming Yu and Michael Vega. 2008. Impedance Track Fuel Gauge Accuracy Test for GSM Phone Applications. *Application Report, SLUA455* (2008).

APPENDIX: ANALYSIS OF OBSERVATION 2

From Eq. (6), we get

$$I^2(t) \cdot r_b \quad = \quad \frac{T_b(t)}{R_b} - \frac{T'_a}{R_b} + C_b \cdot \frac{dT_\mathrm{b}(t)}{dt}, \tag{13}$$

where $\frac{1}{R_b} = \frac{1}{R_a} + \sum_i \frac{1}{R_i}$ and $T'_a = \frac{\frac{T_a}{R_a} + \sum_i \frac{T_i}{R_i}}{\frac{1}{R_a} + \sum_i \frac{1}{R_i}}$. Multiplying R_b to both sides, we have:

$$R_b \cdot r_b \cdot I^2(t) + T'_a = T_b(t) + R_b \cdot C_\mathrm{b} \cdot \frac{dT_\mathrm{b}(t)}{dt}, \tag{14}$$

meaning that the battery temperature will converge at

$$T_\mathrm{b}^{\mathrm{st},1} = R_b \cdot r_b \cdot I^2(t) + T'_a. \tag{15}$$

Combining Eqs. (14) and (15) leads to

$$T_\mathrm{b}^{\mathrm{st},1} = T_b(t) + R_b \cdot C_\mathrm{b} \cdot \frac{dT_\mathrm{b}(t)}{dt}. \tag{16}$$

Multiplying $\frac{1}{R_b \cdot C_b} \cdot e^{\frac{t-t_0}{R_b \cdot C_b}}$ to both sides and taking their integration, we get:

$$\begin{aligned}
\int \frac{1}{R_b \cdot C_b} \cdot e^{\frac{t-t_0}{R_b \cdot C_b}} T_\mathrm{b}^{\mathrm{st},1} \quad &= \quad \int e^{\frac{t-t_0}{R_b \cdot C_b}} \left(\frac{T_b(t)}{R_b \cdot C_b} + \frac{dT_\mathrm{b}(t)}{dt}\right) \\
e^{\frac{t-t_0}{R_b \cdot C_b}} T_\mathrm{b}^{\mathrm{st},1} + C \quad &= \quad \int \left(e^{\frac{t-t_0}{R_b \cdot C_b}} \cdot T_b(t)\right)' \\
T_b^{\mathrm{st},1} + C \cdot e^{-\frac{t-t_0}{R_b \cdot C_b}} \quad &= \quad T_b(t).
\end{aligned} \tag{17}$$

where C is the integration constant. Letting the initial condition be $T_b(t_0) = T_b^{\mathrm{st},0}$, we have $C = T_b^{\mathrm{st},0} - T_b^{\mathrm{st},1}$, and the transient solution is

$$T_b^{\mathrm{tr}}(t) = (T_b^{\mathrm{st},0} - T_b^{\mathrm{st},1}) \cdot e^{-\frac{t-t_0}{R_b \cdot C_b}} + T_b^{\mathrm{st},1}. \tag{18}$$

Thus, the battery temperature equilibrates as an exponential decay process and Observation 2 follows.